Crack Tip Plastic Zone under Mode I Loading and the Non-singular T_{zz}-stress

Yu.G. Matvienko

Mechanical Engineering Research Institute of the Russian Academy of Sciences

Email: ygmatvienko@gmail.com

Abstract: The amplitudes of the second order terms in the three-dimensional series expansion of the crack front stress field are the terms T_{xx} and T_{zz} which describe in-plane and out-of-plane constraint, respectively. All previous analyses of the crack tip plastic zone have ignored the effect of T_{zz} -stress. At the same time, the effect of the T_{zz} -stress on crack tip plastic zones is not revealed heretofore. It is therefore very important to obtain solutions for crack tip plastic zone size taking into account two components of the T-stresses. The present study focus on theoretical and numerical analysis of the joint effect of the non-singular T_{xx} and T_{zz} -stresses on sizes of the plastic zone in the vicinity of the crack tip under mode I loading conditions. The three-dimensional crack tip stresses including T_{xx} and T_{zz} stresses are incorporated into the von Mises yield criteria to develop an expression that models the crack tip plastic zone. Calculations are performed for three thicknesses of the CT specimen. The predicted sizes of the plastic zone in the vicinity of the crack tip of the analysed CT specimens are bounded by sizes of the plastic zones corresponding to two special conditions, namely, plane stress and plane strain. The theoretical results are compared with the results computed by FEM. Theoretical estimations of the plastic deformations zone size with provision for *T*-stress components in whole shows the satisfactory results, especially on line of the crack continuation.

Key words: plastic zone, T_{zz}-stress, mode I crack

1. INTRODUCTION

The different sources of a change in in-plane constraint at the crack tip are associated with crack size, geometry of specimen and type of loading. The source of a change of the out-of-plane crack tip constraint is thickness. To describe in-plane and out-of-plane constraint effects in fracture analysis, the following parameters can be used, namely, T_z-parameter [1], local triaxiality parameter *h* [2] and the non-singular terms in William's series expansion of the crack tip stress fields [3].

These parameters considerably influence on the fracture toughness [4-8]. Not emphasize attention on advantages and disadvantages of the above-mentioned constraint parameters, we concentrate on the non-singular components of the *T*-stresses at the crack tip. The second order terms T_{xx} and T_{zz} in William's series expansion are defined as T-stresses, and they are the only non-zero and non-singular terms. It should be noted that T_{xx} has been simply referred to as T-stress. T_{xx} and T_{zz} represent the stresses in the crack surface plane normal to and tangential to the crack front, respectively.

In a two-dimensional (2D) crack configuration, T_{zz} is related to T_{xx} by $T_{zz} = \nu T_{xx}$ under plane strain conditions, where ν is Poisson's ratio. It is well-known that the sign and magnitude of the T_{xx}-stress substantially change the size and shape of the plane strain crack tip plastic zone [9-11]. Therefore, the T_{xx}-stress has been used to characterize the effect of in-plane constraint on the crack tip plastic zone.

The amplitudes of the second order terms in the three-dimensional series expansion of the crack front stress field are the terms T_{xx} and T_{zz} which describe in-plane and out-of-plane constraint, respectively. All previous analyses of the crack tip plastic zone have ignored the effect from T_{zz}-stress. At the same time, the effect of the T_{zz}-stress on crack tip plastic zones is not revealed heretofore. It is therefore very important to obtain solutions for crack tip plastic zone size taking into account two components of the T-stresses.

The present paper focuses on theoretical and numerical analysis of the joint effect of the non-singular T_{xx} and T_{zz}-stresses on sizes of the plastic zone in the vicinity of the crack tip under mode I loading conditions.

2. THEORETICAL ANALYSIS OF THE PLASTIC ZONE

2.1. Modeling of the plastic zone

The general form of the linear elastic crack tip stress fields within a three-dimensional crack problem can be characterized by the singular (the first order term) and the nonsingular terms (second order terms) [3]

$$\sigma_{xx} = \frac{K_I}{\sqrt{2\pi \cdot r}} \cdot \cos\frac{\theta}{2} \cdot \left(1 - \sin\frac{\theta}{2} \cdot \sin\frac{3\theta}{2}\right) + T_{xx} + \ldots, \quad (1)$$

$$\sigma_{yy} = \frac{K_I}{\sqrt{2\pi \cdot r}} \cdot \cos\frac{\theta}{2} \cdot \left(1 + \sin\frac{\theta}{2} \cdot \sin\frac{3\theta}{2}\right) + \ldots, \quad (2)$$

$$\sigma_{zz} = 2\nu \cdot \frac{K_I}{\sqrt{2\pi \cdot r}} \cdot \cos\frac{\theta}{2} + T_{zz} + \ldots, \quad (3)$$

$$\tau_{xy} = \frac{K_I}{\sqrt{2\pi \cdot r}} \cdot \cos\frac{\theta}{2} \cdot \sin\frac{\theta}{2} \cdot \cos\frac{3\theta}{2} + \ldots, \quad (4)$$

$$\tau_{yz} = 0, \ \tau_{zx} = 0. \quad (5)$$

Here, r and θ are the in-plane polar coordinates of the plane normal to the crack front centered at the crack tip with $\theta = 0$ corresponding to a line ahead of the crack (Fig. 1), σ and τ are the normal and shear stress respectively, K_I is the mode I stress intensity factor (SIF), E is Young's modulus, ν is Poisson's ratio. The singular term corresponds to the stress intensity factor. The terms T_{xx} and T_{zz} are the amplitudes of the second order terms in the three-dimensional series expansion of the crack front stress field in the *x* and *z* directions, respectively. These terms characterize corresponding crack tip constraint along above-mentioned axes.

The T_{xx}-stress component can be calculated from equations (1) and (2) as difference between σ_{xx} and σ_{yy} stresses very near the crack front. The value of T_{zz}-stress components is defined according to the following relationship [4]

$$T_{zz} = E \cdot \varepsilon_{zz} + \nu \cdot T_{xx}. \quad (6)$$

where ε_{zz} is strain along the crack front.

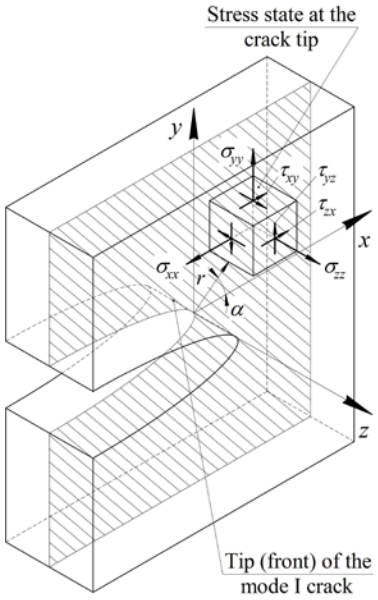

Figure 1: Three-dimensional coordinate system for the region along the crack front

In the case of plane stress conditions (2D stress state), stress component $\sigma_{zz} = 0$. For plane strain conditions, stress component σ_{zz} is equal to

$$\sigma_{zz} = \nu\left(\sigma_{xx} + \sigma_{yy}\right) = 2\nu \cdot \frac{K_I}{\sqrt{2\pi \cdot r}} \cdot \cos\frac{\theta}{2} + \nu \cdot T_{xx}\,. \qquad (7)$$

In the present work, the plastic zone ahead of the crack tip is determined by the von Mises yield criterion

$$\left(\sigma_{xx} - \sigma_{yy}\right)^2 + \left(\sigma_{yy} - \sigma_{zz}\right)^2 + \left(\sigma_{zz} - \sigma_{xx}\right)^2 + 6\left(\tau_{xy}^2 + \tau_{yz}^2 + \tau_{zx}^2\right) = 2\sigma_Y^2 \qquad (8)$$

where σ_Y is the yield stress.

Substituting of equations (1)-(5) into the von Mises yield criterion (8), the crack tip plastic zone size $r = r_p$ can be estimated. After comprehensive mathematical manipulations, the solution for r_p as a function of θ and the T-stress components is given by the following formula

$$\frac{1}{2\pi \cdot r_p} \cdot \left(K_I^2 \cdot \left(A_I + \frac{D_I}{K_I} \cdot \sqrt{r_p} \right) \right) = 2\sigma_Y^2\,. \qquad (9)$$

The joint effect of the non-singular T_{xx} and T_{zz}-stresses on sizes of the plastic zone in the vicinity of the crack tip under mode I loading conditions is included into basic Eq. (9).

The parameters in Eq. (9) are denoted as follows

$$D_I = \sqrt{\frac{\pi}{2}} \cdot \left(\begin{array}{l} \left(\cos\frac{\theta}{2} + 3\cos\frac{5\theta}{2} \right) \cdot T_{xx} - 8\nu \cdot \cos\frac{\theta}{2} \cdot \left(T_{xx} + \frac{T_{zz}}{\nu} \right) + \\ + 16\nu \cdot \cos\frac{\theta}{2} \cdot \left(T_{zz} \right) \end{array} \right), \quad (10)$$

$$A_I = \left(1-2\nu\right)^2 \cdot \left(1+\cos\theta\right) - \frac{3}{4} \cdot \left(\cos 2\theta - 1\right). \quad (11)$$

Equation (9) can be solved to determine the angular distribution of the plastic zone size in the vicinity of the crack tip

$$r_p(\theta)_{1,2} = \frac{1}{4U^2} \cdot \left[V \pm \sqrt{V^2 + 4U \cdot W} \right]^2, \quad (12)$$

where parameters *U*, *V*, *W* are

$$U = 4\pi \cdot \sigma_Y^2, \quad V = K_I \cdot D_I, \quad W = K_I^2 \cdot A_I. \quad (13)$$

Finally, solution (12) can be written in more representative form

$$r_p(\theta)_{1,2} = \left[\frac{K_I^2}{\pi \cdot \sigma_Y^2} \right] \cdot \left[\frac{D_I \pm \sqrt{D_I^2 + \left(16\pi \cdot \sigma_Y^2\right) \cdot A_I}}{2 \cdot \sqrt{16\pi \cdot \sigma_Y^2}} \right]^2. \quad (14)$$

It can be shown that special solution for the crack tip plastic zone in the case of plane strain conditions under mode I loading follows from general solution (12) (e.g., [11]):

$$U = 4\pi \cdot \sigma_T^2, \quad V = K_I \cdot E_I, \quad W = K_I^2 \cdot B_I. \quad (15)$$

Here, the additional coefficients are

$$B_I = \left(1-2\nu\right)^2 \cdot \left(1+\cos\theta\right) - \frac{3}{4} \cdot \left(\cos 2\theta - 1\right). \quad (16)$$

$$E_I = \sqrt{\frac{\pi}{2}} \cdot \left(\begin{array}{l} \left(\cos\frac{\theta}{2} + 3\cos\frac{5\theta}{2} \right) \cdot T_{xx} - 8\nu \cdot \cos\frac{\theta}{2} \cdot \left(2T_{xx} \right) + \\ + 16\nu \cdot \cos\frac{\theta}{2} \cdot \left(\nu \cdot T_{xx} \right) \end{array} \right). \quad (17)$$

For plane stress conditions, the angular distribution of the plastic zone at the mode I crack tip can be calculated from (12) taking into account the following coefficients

$$U = 4\pi \cdot \sigma_T^2,\ V = K_I \cdot F_I,\ W = K_I^2 \cdot C_I, \tag{18}$$

$$C_I = (1+\cos\theta) - \frac{3}{4}\cdot(\cos 2\theta - 1). \tag{19}$$

$$F_I = \sqrt{\frac{\pi}{2}} \cdot \left(\left(\cos\frac{\theta}{2} + 3\cos\frac{5\theta}{2} \right) \cdot T_{xx} \right). \tag{20}$$

It should be noted that equation (12) has to meet certain conditions, namely

$$V^2 + 4U \cdot W^2 \geq 0 \text{ и } U \neq 0. \tag{21}$$

If above-mentioned inequalities (21) satisfy, sizes of the crack tip plastic zone are calculated as

$$r_{p_1} = \frac{V + \sqrt{V^2 + 4U \cdot W}}{2U},\ r_{p_2} = \frac{V - \sqrt{V^2 + 4U \cdot W}}{2U}. \tag{23}$$

The value of r_{p_1} is positive in the wide range of coefficients *U*, *V*, *W* and should be used in all calculations. At the same time value of r_{p_2} has a negative sign.

2.2. The effect of thickness on the plastic zone

For the 3D model, the CT specimen is considered. The plastic zone is analyzed for a wide range of the ratio *B/W*=0.25-0.5 within the limits of the pure plane stress and pure plane strain conditions. The stress intensity factor K_{max} of experimental specimens of Steel JIS S55C is 66 MPa·m$^{1/2}$, corresponding values of the *T*-stress components are presented in table 1[7]. The T-stress components are calculated along the plastic zone boundary on the line of the crack extension. According with slight variation of the T_{xx}-stresses for the CT specimens with different ratio *B/W*, the value of T_{xx}-stresses has been assumed to be constant and equal to 182 MPa.

The fracture tends to initiate at the specimen thickness center, the values of the crack tip plastic zone size at specimen thickness center were chosen to represent the characteristic intensity of these values. The predicted results of the angular distribution of the plastic zone sizes in the vicinity of the crack tip at the specimen thickness centre for the CT specimens with various thicknesses to width ratio are given in Fig. 2. To determine the validity of the plastic zone model derived above, basic equation is applied to a pure

mode I situation under plane strain conditions, and the results agree with published solutions [9, 11].

Table 1: The T-stress components on the line of the crack extension (boundary of the plastic zone)

B/W	***0,25***	***0,40***	***0,50***
T_{xx}, MPa	***186.59***	***182.36***	***176.28***
T_{zz}, MPa	***-159.47***	***-106.81***	***-84.97***

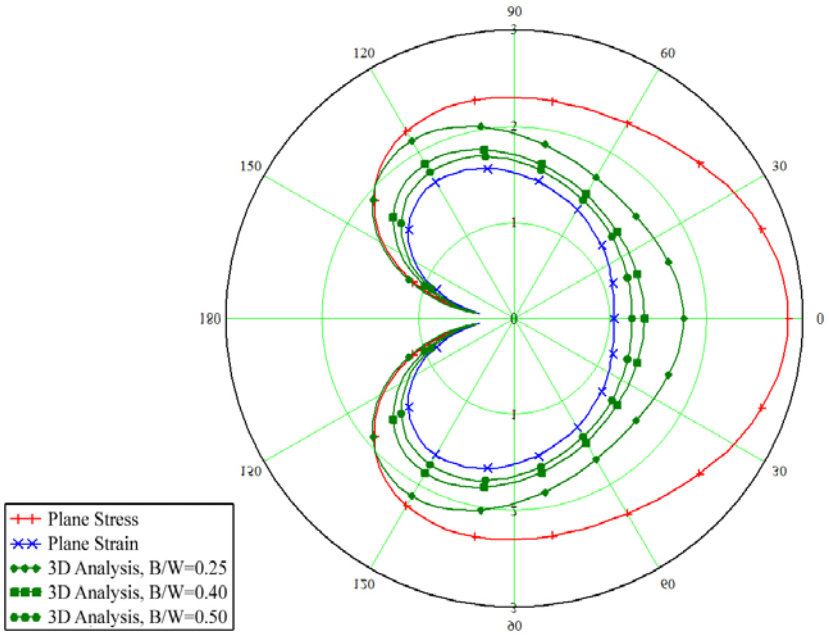

Figure 2. The angular distribution of the plastic zone size at the specimen thickness centre of the CT specimens

The predicted sizes of the plastic zone in the vicinity of the crack tip of the analysed CT specimens are bounded by sizes of the plastic zones corresponding to two special conditions, namely, plane stress and plane strain. Moreover, the shape and size of the plastic zones tend to typical plastic zones for plane strain conditions, when specimen thickness increases. Thus, the results confirm the necessity to take into account the constraint effect at the crack tip on the plastic zone by means of both non-singular stresses T_{xx} and T_{zz}.

3. NUMERICAL MODELLING THE PLASTIC ZONE

3.1. Finite Element Analysis

To demonstrate the validity of the plastic zone model, finite element analysis was conducted.

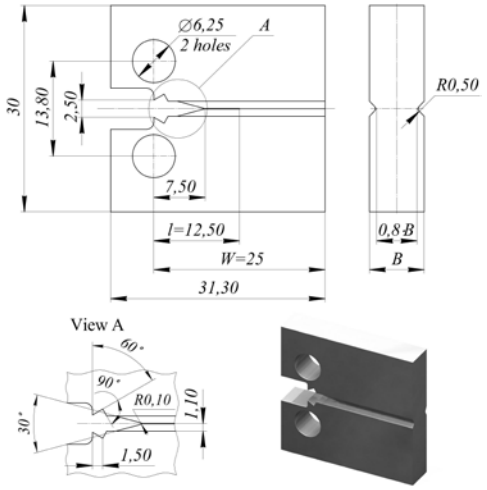

Figure 3: The geometrical model of the CT specimen

It is well-known that the creation of the calculation model lies in the basis of numerical experiment. Primary tasks, which are being solved for this purpose, are the following. First of all, the solid-state geometrical model of the CT specimen (fig. 3) is created in the modern CAD system. Three geometrical models with the ratio B/W = 0,25, B/W = 0,40 и B/W = 0,50 are prepared for an analysis of the effect of the T-stress components on the plastic zone. Deviation from the figure was that the crack length a, was set at the nominal value of 12.5 mm (a/W= 0.5) for all cases.

The finite element model of the CT specimen is represented in Fig. 4. For the reason of minimization of the required computing resources finite element mesh was created on the one half of the geometric model (fig. 4). For more detailed account of the stress and strain distribution at the crack tip the local mesh concentration with diameter 10 mm was created around crack tip.

Spatial finite element mesh was created in one of the modern CAE system by means of decomposition of the internal volume of the geometrical model to the finite number of the small calculation elements having spatial polygon shape. Parabolic elements (the second order elements) with tetrahedral shape and one intermediate node along each side were used in this numerical analysis. The use of such elements allows achieving greater calculation accuracy due to more accurate

reproduction of the curvilinear surfaces of the geometric model, as well as more accurate shape function which connects displacement of the arbitrary point of the calculation element with displacement of its nodes.

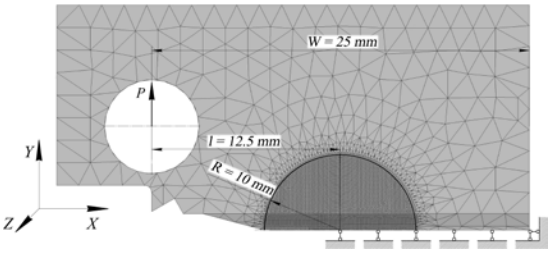

(a) Two- dimensional global mesh

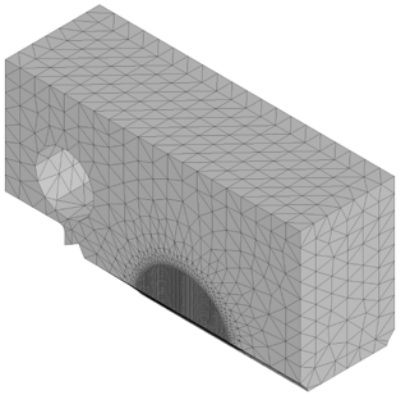

(b) Three-dimensional global mesh

Figure 4: Finite element model of the CT specimen.

The creation of the load system is made in the modern CAE system. Fixed values of the vertical forces (force *P*) were added to the nodes situated on the cylindrical surface of the specimen hole. The value of K_{max} in the table 2 was obtained as the stress intensity factor corresponding to the maximum load P_{max} from the well-known equation in ASTM E399.

Table 2: Loading conditions of the CT specimen

	B/W=0,25	***B/W =0,40***	***B/W =0,50***
P_{max}, ***kN***	***6,0***	***9,6***	***12,0***
K_{max}, $MPa \cdot m^{1/2}$	***66,0***	***66,0***	***66,0***

Finite element calculations allow analyzing size and shape of the plastic zone in the vicinity of the crack tip by means of diagrams of the von Mises equivalent stresses.

3.2. Algorithm for the processing of results of the numerical modeling

Sizes and shape of the plastic zone were analyzed using the image data of the distribution of equivalent von Mises stresses in the vicinity of the crack tip.

Estimation of the influence of the *T*-stress components on the plastic zone size is made in the mathematical package, for what special algorithm is created for processing the computed diagrams (Fig. 5). These diagrams must satisfy certain graphic conditions. The diagram must present itself as monochrome images of the equivalent stress fields with clear gray gradation of stress from white (stress level equal to yield stress σ_Y) to black (zero stress level). In according with the main idea of algorithm the special procedure realizes consequent selection of pixels, which belongs to the image of the current diagram, along radius from the crack tip with appropriate step. If the color of current pixel differs from white, the procedure of pixel selection is stopped and current values of radius and angle are saved. This radius corresponds to the boundary of the plastic zone in the vicinity of the crack tip.

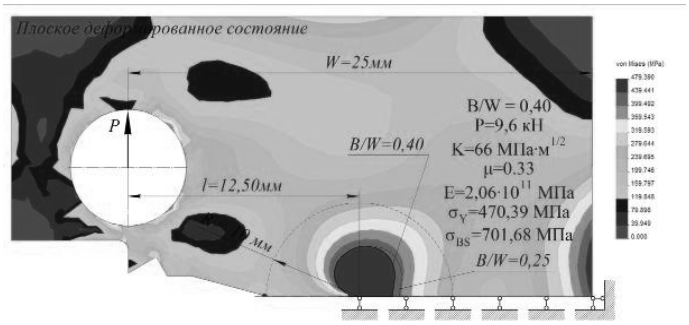

Figure 5: Typical image data of the distribution of equivalent von Mises stresses in the vicinity of the crack tip of the CT specimen

4. DISCCUSSION

In according with the above-mentioned methodology for theoretical estimation of the plastic zone size, the predicted results are compared with the results computed by FEM. Comparison of theoretical and FEM results of the plastic zone size estimation at the CT specimen thickness is presented at Fig. 6.

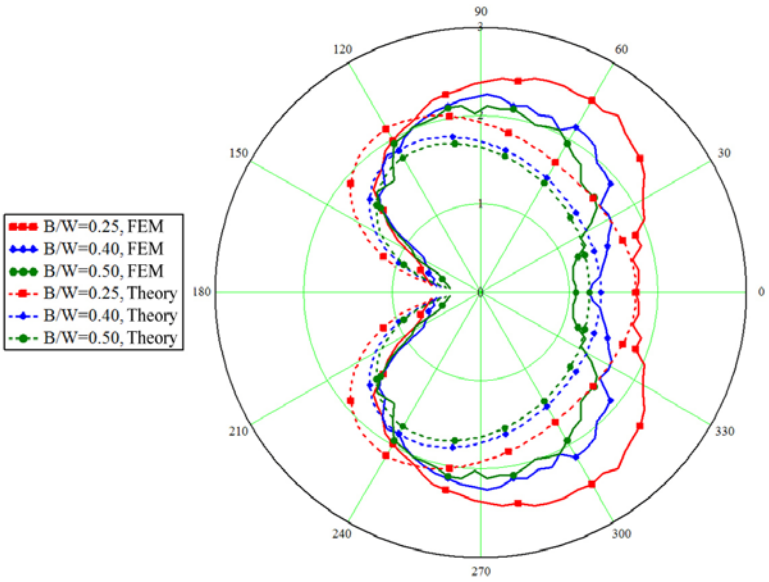

Figure 6: Comparison of theoretical and FEM results of the plastic zone estimation at the CT specimen thickness

It is observed that deviation of the theoretical plastic zone sizes from the FEM results does not exceed 20% in angular intervals (0°, 30…45°) and (90°…100°,135°…145°) (Fig. 7). Deviation achieves maximum and exceeds 40% in angular intervals from 135°…145° to 180° that can be connected with particularity of the algorithm which is used during processing of the equivalent von Mises stress diagrams.

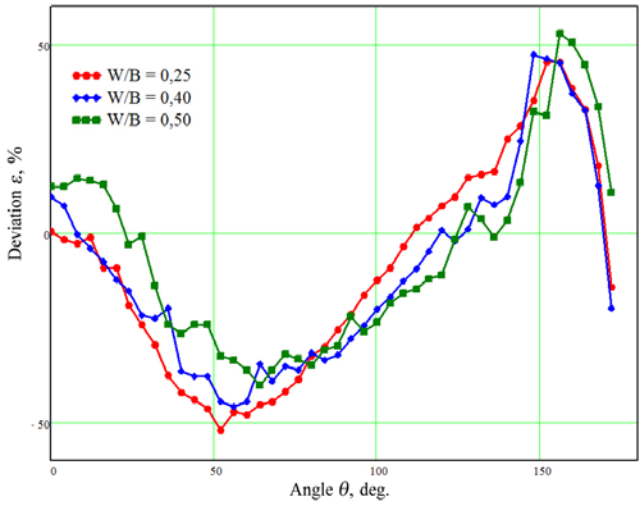

Figure 7: Deviation of the theoretical plastic zone sizes from the FEM results

Probably, so high divergence between results of the numerical experiment and analytical calculation in interval (0°…145°) can be explained that actually T-stresses are not a constant and depend on angle θ. This assumption is corroborated by the results of the FEM analysis (Fig. 8, Fig. 9).

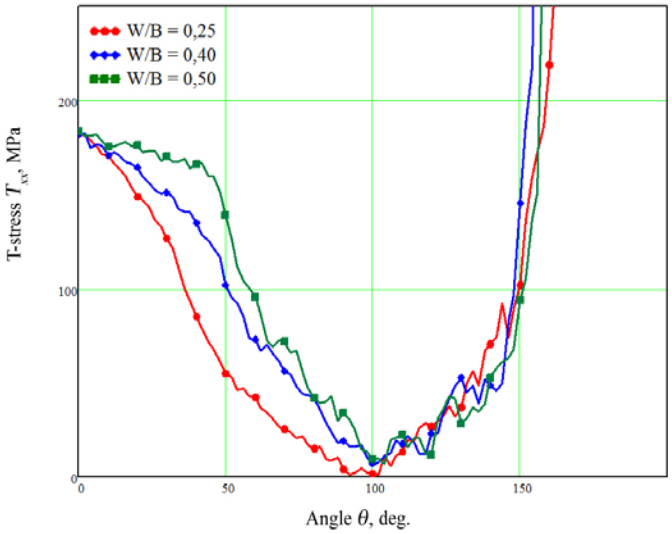

Figure 8: Finite Element estimation of angular distribution of the T_{xx}-stress along the boundary of the plastic deformations zone at the specimen thickness centre

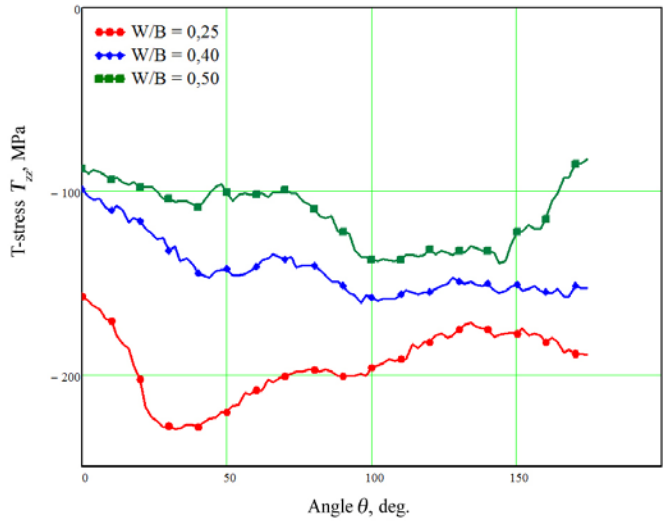

Figure 9: Finite Element estimation of angular distribution of the T_{zz} -stress along the boundary of the plastic deformations zone at the specimen thickness centre

We can receive evidence that dependence between *T*-stress components and angular coordinate exists if we will express K_I from equation (2) and substitute received relation to the equation (1). As a result we will receive angular distribution of T_{xx}:

$$T_{xx} = \sigma_{xx} - \sigma_{yy} \cdot \left(\frac{3\cos\frac{\theta}{2} + \cos\frac{5\theta}{2}}{5\cos\frac{\theta}{2} - \cos\frac{5\theta}{2}} \right). \qquad (27)$$

In similar manner we can receive angular distribution of T_{zz}:

$$T_{zz} = \sigma_{zz} - \nu \left(\sigma_{yy} \cdot \left(\frac{8\cos\frac{\theta}{2}}{5\cos\frac{\theta}{2} - \cos\frac{5\theta}{2}} \right) + T_{xx} \right). \qquad (28)$$

Received relations confirm made early assumptions about necessity of the introduction into asymptotic formulas (1) and (3) angular distributions of components of the nonsingular stresses.

5. CONCLUSIONS

The theoretical analysis of the joint influence of the nonsingular components of the *T*-stresses on the size of the plastic deformations zone at the tip of the mode I crack is carried out with attraction of asymptotic formulas, which taking into account triaxiality of the stress state at the tip of the mode I crack and Mises yield criterion.

The size of the plastic zone at the middle surface of the specimen decreases during increasing of the specimen thickness. It reflects the increasing of the deformations constraint degree at the crack tip by means of increasing of nonsingular stress T_{zz}.

Theoretical estimations of the plastic zone size with provision for *T*-stress components in whole shows the satisfactory results, especially on line of the crack continuation. This is especially important in case of estimation of the reliable values of the fracture toughness. However, in some cases divergence between analytical calculation and FEM results exceeds 20%. For more correct determination of the shape of the plastic deformations zone it is necessary to take into account angular distribution of the nonsingular *T*-stresses at the crack tip.

Certainly, accurate analysis and estimation of the plastic zone sizes at the mode I crack tip will promote the development of more correct criterions of validity in estimation of the fracture toughness of engineering materials.

REFERENCES

1. W. Guo. Three-dimensional analyses of plastic constraint for through-thickness cracked bodies. *Engineering Fracture Mechanics*, 62: 383-407, 1999.
2. B.S. Henry and A.R. Luxmoore. The stress triaxiality constraint and the Q-value as ductile fracture parameter. *Engineering Fracture Mechanics*, 57: 375-390, 1997.
3. T. Nakamura and D. M. Parks. Determination of elastic T-Stress along three-dimensional crack fronts using an interaction integral. *International Journal of Solids and Structures*, 29:1597-1611, 1992.
4. W.A. Sorem, R.H. Dodds and S.T. Rolfe. Effects of crack depth on elastic plastic fracture toughness. *International Journal of Fracture*, 47: 105–126, 1991.
5. S. Liu and Y.J. Chao. Variation of fracture toughness with constraint. *International Journal of Fracture*, 124: 113-117, 2003.
6. X.K. Xhu and Y.J. Chao. Specimen size requirements for two-parameter fracture toughness testing. *International Journal of Fracture*, 135: 117–136, 2005.
7. T. Meshii and T. Tanaka. Experimental T_{33}-stress formulation of test specimen thickness effect on fracture toughness in the transition temperature region. *Engineering Fracture Mechanics*, 77: 867-877, 2010.
8. H.M. Meliani, Yu.G. Matvienko and G. Pluvinage. Two-parameter fracture criterion ($K_{\rho,c}$-$T_{ef,c}$) based on notch fracture mechanics. *International Journal of Fracture*, 167: 173-182, 2011.
9. J.R. Rice. Limitations to the-scale yielding approximation for crack-tip plasticity. *Journal of the Mechanics and Physics of Solids*, 22: 17-26, 1974.
10. S.G. Larsson and A.J. Carlsson. Influence of non-singular stress terms and specimen geometry on small-scale yielding at crack tips in elastic-plastic materials. *Journal of the Mechanics and Physics of Solids*, 21: 263-278, 1973.
11. Q. Nazarali and X. Wang. The effect of T-stress on crack-tip plastic zones under mixed-mode loading conditions. *Fatigue and Fracture of Engineering Materials and Structures*, 34: 792–803, 2011.